

# Evaluation of Pendrin Expression Using Nuclear Imaging Modalities and Immunohistochemistry in Animal Thyroid Cancer Model

## Abstract

**Context:** The impaired ability of thyroid cancer (TC) cells to uptake and concentrate iodine represents a major therapeutic challenge in malignant TC management. This has been reported probably due to reduced or loss of expression of pendrin in thyroid tumors. **Aims:** In view of this, we evaluated the pendrin expression in the chemically induced (using N-bis[2-hydroxypropyl] nitrosamine [DHPN]) TC model in Wistar rats. **Methods:** Uptake in the thyroid gland was evaluated by positron emission tomography with computed tomography (PET-CT) and scintigraphy imaging. Further histopathology (HP) and immunohistochemistry (IHC) were performed for confirming malignancy. **Results:** The altered uptake in the thyroid gland was observed by PET-CT and scintigraphy imaging. Significant pathological changes in the thyroid were observed using 2-deoxy-2-(fluorine-18) fluoro-D-glucose PET-CT, technetium-99m pertechnetate imaging, and reduced iodine-131 uptake ( $n = 4$ ) in DHPN-induced animals compared to control indicative of thyroid cell proliferation. In treated groups, tissue HP revealed hyperplastic follicular to papillary cell proliferation with variable mitotic activity. The malignant nature of the tissue and variable uptake of the tracer were further reconfirmed by IHC. IHC revealed reduced pendrin expression in malignant thyroid tissue. **Conclusions:** Hence, nuclear imaging techniques can be of aid in the early identification and evaluation of cellular changes during the early development of tumor models in laboratory animals. In conclusion, our study reveals that pendrin expression plays a vital role in thyroid uptake, and its reduction was observed in TC in a chemically induced TC model.

**Keywords:** Fluorine-18 fluoro-D-glucose positron emission tomography with computed tomography, immunohistochemistry, iodine-131 uptake, N-bis(2-hydroxypropyl) nitrosamine, pendrin, technetium-99m pertechnetate scintigraphy, thyroid cancer animal model, Wistar rats

## Introduction

Thyroid cancer (TC) represents approximately 95% of all endocrine tumors, accounting for roughly 3% of all cancers diagnosed annually worldwide. Most carcinomas in the thyroid, defined as papillary thyroid carcinoma (PTC), follicular thyroid carcinoma (FTC), and Hürthle cell carcinoma, are well-differentiated tumors originating from the follicular cells with an incidence of about 79%, 13%, and 15%, respectively, in humans. Whereas medullary thyroid carcinoma which arises from the parafollicular “C” cells and anaplastic thyroid carcinoma (ATC) which is an undifferentiated subtype of TC account for 4% and 2%, respectively. Poorly differentiated TC (DTC) is a rare subtype of TC placed biologically between PTC or FTC and ATC, with an incidence of around 2%–15% of all thyroid malignancies.<sup>[1]</sup>

This is an open access journal, and articles are distributed under the terms of the Creative Commons Attribution-NonCommercial-ShareAlike 4.0 License, which allows others to remix, tweak, and build upon the work non-commercially, as long as appropriate credit is given and the new creations are licensed under the identical terms.

For reprints contact: WKHLRPMedknow\_reprints@wolterskluwer.com

Radioactive iodine (RAI) iodine-131 (I-131) is fundamental in routine adjuvant management in patients with high-risk DTC. Nonetheless, 5%–15% of DTC and 50% of metastatic DTCs are RAI-refractory (RAI-R) to therapy. Thus, RAI-R TC patients have poor outcomes, with 5-year disease-specific survival rates of 60%–70%. Whereas those with RAI-R metastatic TC have the worst outcomes, with a 10-year survival rate of up to 10%. RAI-R most often develops in the background of a loss of thyroid differentiation features.<sup>[2]</sup> Sodium-iodide symporter (NIS) and pendrin, functioning as iodide ( $I^-$ ) transporters, are proteins found principally, but not exclusively, in the thyroid tissue.<sup>[3]</sup> One of the known hallmarks of dedifferentiation is attributed to the impairment of NIS function.<sup>[2]</sup> Pendrin, a 110 kDa glycoprotein, encoded by the Pendred syndrome (PDS) gene, is a member of the *SLC26A4* gene family.

**How to cite this article:** Gholve CS, Shete Y, Rakshit S, Kulkarni S. Evaluation of pendrin expression using nuclear imaging modalities and immunohistochemistry in animal thyroid cancer model. Indian J Nucl Med 2023;38:328-33.

**Chandrakala Sanjay Gholve,  
Yogita Shete,  
Sutapa Rakshit,  
Savita Kulkarni**

Radiation Medicine Centre,  
Bhabha Atomic Research  
Centre, Mumbai, Maharashtra,  
India

**Address for correspondence:**  
Dr. Savita Kulkarni,  
Radiation Medicine Centre,  
Bhabha Atomic Research  
Centre, TMH Annexe,  
Parel, Mumbai - 400 012,  
Maharashtra, India.  
E-mail: savitapk@barc.gov.in

Received: 03-04-2023  
Revised: 19-05-2023  
Accepted: 29-05-2023  
Published: 20-12-2023

### Access this article online

Website: [www.ijnm.in](http://www.ijnm.in)

DOI: 10.4103/ijnm.ijnm\_46\_23

### Quick Response Code:



It is an anion transporter that is predominantly expressed in the inner ear, thyroid, and kidney. In thyroid cells, pendrin is involved in the apical iodide efflux from the follicular epithelium to the follicular lumen where organification of iodide takes place.<sup>[4]</sup> The occurrence and level of pendrin expression and iodide efflux are regulated by thyroid transcription factor 1, thyroid-stimulating hormone (TSH), and thyroglobulin, while iodide itself does not have a major effect on pendrin gene expression.<sup>[3]</sup> On the contrary, Calil-Silveira *et al.*<sup>[5]</sup> showed that acute iodide treatment increased *SLC26A4* mRNA content, in both *in vitro* and *in vivo* models. Although pendrin is suggested to be an apical iodide transporter in the thyroid, the expression and localization of pendrin in diseased thyroids have not been adequately investigated.<sup>[6]</sup> However, the pendrin gene has been previously reported to be linked with autoimmune thyroid diseases.<sup>[7]</sup> The diagnostic and therapeutic uses of radioiodine in the management of TCs, however, are often hampered by the impaired ability of the TC cells to uptake and concentrate iodine. This represents a major therapeutic challenge in TC management. The retention time of radioiodide in thyrocytes is determined by I<sup>-</sup> uptake and I<sup>-</sup> efflux.<sup>[4]</sup> Hence, numerous efforts are being made to improve the efficiency of RAI uptake and retention in patients with RAI refractory TC.<sup>[2]</sup> Several studies have reported decreased or even absence of expression of pendrin, in many thyroid tumors, demonstrating a pathological role of pendrin in the impairment of the iodide-concentrating mechanism of TC cells.<sup>[8,9]</sup> A reciprocal relationship between methylation and expression of the *SLC26A4* gene was shown in cell lines and thyroid tissues.<sup>[10]</sup> These data provide further evidence supporting the clinical use of demethylating agents to improve the efficiency of radioiodine treatment for TC patients in the near future. Nevertheless, this hypothesis deserves extensive testing in the clinical setting. Therefore, the study of pendrin expression in pathological thyroid tissues, particularly in cancerous tissues, is of interest due to its iodide translocating activity, which serves as one of the iodide suppliers for organification processes.

In view of this, the present work was planned as a preclinical pilot study that focused on the development of a chemically induced TC animal model using N-bis (2-hydroxypropyl) nitrosamine (DHPN). Different preclinical animal models such as rodents and transgenic animals have the potential to carry out such kinds of studies. Conversely, the low survival rate, high cost, efforts, ethical issues, and availability hamper the utility of transgenic animals.<sup>[11]</sup> Hence, the chemically induced Wistar rat model was focused for the present study. Further, the genetic alterations have been identified in chemically induced rodent models of cancer that mimic the changes present in human cancer in terms of stages of initiation and progression from premalignancy to neoplasia seen in the

earlier scientific report. However, the natural occurrence and tumorigenesis are often unknown and may be different between the rat, mice, and human species. Wistar rat is the most commonly used model in chemical carcinogen testing due to its susceptibility to carcinogens.<sup>[12]</sup>

DHPN is a chemical with the ability to stimulate thyroid proliferation and convert it into adenoma or carcinoma.<sup>[13]</sup> It is a potent chemical mutagen and wide-spectrum carcinogen that induces different types of tumors, including TC of both sexes in various rat strains.<sup>[14]</sup>

In our study, a Wistar rat was selected as a preclinical animal model for TC development, and PDS expression was correlated with nuclear imaging modalities and further confirmed by immunohistochemistry (IHC). Post-DHPN induction, pathological changes in the thyroid were observed using positron emission tomography with computed tomography (PET-CT) and scintigraphy imaging methods. Further, sequential evaluation of histopathological and immunohistochemical characteristics of thyroids in rats was executed to elucidate the mechanisms of progression to invasive carcinomas and was correlated with pendrin protein expression.

## Methods

### Animal studies and treatments

The animal experiments were carried out following the protocols/guidelines previously approved by the Committee for Control and Supervision of Experiments on Animals, India. A total of 18 male (270–280 g) 8-week-old healthy inbred Wistar strain rats were kept on *ad libitum* of commercial pelleted feed/diet and filtered drinking water (purified by ultraviolet and reverse osmosis) throughout the experiments and were maintained at a controlled temperature of 23°C ± 1°C, humidity of 55% ± 5%, and in a 12 h light/12 h dark cycle. Experimental animals were kept for a quarantine period of 10 days before the start of the experiment. The animals were grouped into two groups based on their body weights. Group 1 (treatment group animals, *n* = 12) and Group 2 (control animals, *n* = 6) animals. Group 1 (treatment group) was injected with DHPN obtained from MedChem, UK (catalog number 53609-64-6), and the dose was referred from Hiasa *et al.*, in 1991,<sup>[15]</sup> with a slight modification at a dose rate of 83 mg/animal by the intraperitoneal route (*i/p*), fortnightly, for 110 days; whereas Group 2 (control group) animals received only normal saline, and posttreatment animals were subjected to tumor development analysis. Radioactivity-injected animals were taken care by providing food and water, and changing the cage under the supervision of the Radiation Safety Officer (RSO). Disposal of radioactive animal carcass was allowed to store in cold storage following delay and decay procedures and further monitored by the RSO before its disposal.

### Animal positron emission tomography with computed tomography imaging and scintigraphy imaging

Five weeks post DHPN treatment, six animals from Group 1 (DHPN treatment) and three from Group 2 (control) each were injected (intravenously) with approximately 400  $\mu\text{Ci}$  2 deoxy 2 (fluorine 18) fluoro D glucose (F 18 FDG) and subjected to F-18 FDG PET-CT scan under Gemini TF 16 Slice PET-CT camera. The data were reconstructed using the RAMLA reconstruction algorithm. Further, six animals from Group 1 (DHPN treatment) and three from Group 2 (control) each were injected (intravenously) with approximately 400  $\mu\text{Ci}$  technetium-99m pertechnetate ( $\text{Tc-99m}$  pertechnetate) scintigraphy imaging under dual head GE Infinia gamma camera. Sequential static imaging was done in a  $265 \times 256$  matrix size, zoom 2, with 350 Kcts–500 Kcts using a standard acquisition protocol (Serview: 90 KV, 20 MA, CT: 120 KV, 80 mA, PET: 1 min emission/bed) using F-18 FDG radiopharmaceutical. Animal imaging was done under anesthesia using ketamine (80 mg/kg body weight) and xylazine (5 mg/kg body weight) by the i/p route. Uptake analysis was done with the help of software for the evaluation of disease initiation and its propagation.<sup>[16]</sup> After 17 weeks, the metabolic alteration in the thyroid gland was checked by giving I-131 (8  $\mu\text{Ci}$ ) orally, and imaging for thyroid uptake study was done at different time points: 2 h, 24 h, and 48 h. The analysis of the uptake was done by a camera-based method with reference to the I-131 standard source. The experimental timeline is schematically depicted in Figure 1.

### Necropsy and histopathological observations

Terminal sacrifice was done at 20 weeks, and all vital organs and thyroid tissues were collected for histopathology (HP) and IHC. The bilateral thyroid lobes were excised and fixed in 10% neutral buffer formaldehyde and routinely embedded in paraffin. Tissue sections of 3–5  $\mu\text{m}$  were prepared for staining with hematoxylin and eosin (H and E) stain. Different pathological changes in the thyroid gland were estimated by light microscopic analysis. According to the published criteria, focal proliferative lesions of the follicular epithelial cells were classified in H and E-stained sections as focal hyperplasia, adenomas, intrathyroidal carcinomas, and invasive carcinomas to the thyroid capsule or adjacent tissues.<sup>[17]</sup>

### Immunohistochemistry

The thyroid section was subjected to IHC using a specific purified primary polyclonal anti-pendrin antibody (Thermo Fisher Scientific, Cat. no. PA5-42060 SLC26A4) for the evaluation of the pendrin expression. IHC was done using an indirect method of staining<sup>[6]</sup> using fluorescent dye for pendrin expression. Microscopic evaluation was performed using a fluorescent microscope (Inverted Leica DMi8 S).

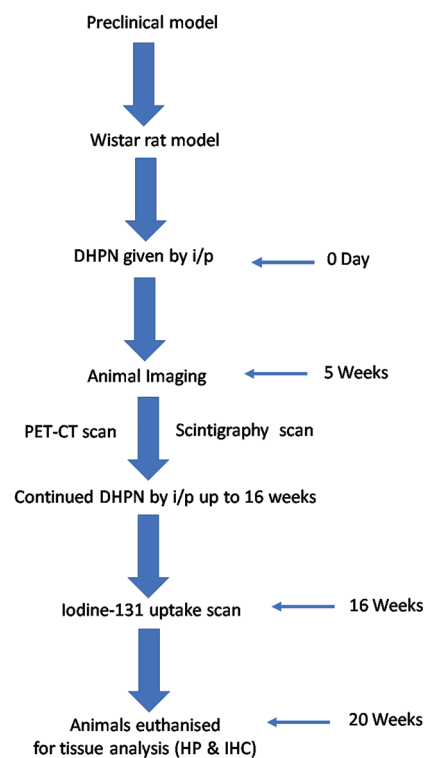


**Figure 1: Schematic diagram of experimental timeline.** DHPN: N-bis (2-hydroxypropyl) nitrosamine, PET-CT: Positron emission tomography with computed tomography, HP: Histopathology, IHC: Immunohistochemistry

### Statistical analysis

All data are reported as means  $\pm$  standard deviation. The *t*-test was used to determine the difference between the treatment group (DHPN) and the control group. The significance level was set at 5% ( $P < 0.05$ ).

### Results and Discussion

Chemically induced tumor model development is possible in rodents with many chemicals like DHPN, urethane, tobacco-related carcinogens, transgenic, or a combination.<sup>[18]</sup> The thyroid tumor model was seen in rats at 110 days posttreatment; however, a variable development period has been reported in the literature.<sup>[19]</sup> This could be due to variations in the dose and route of administration used in the study. The changes in the thyroid may have occurred due to the promotion of growth stimulation by the elevation of serum TSH and propagation with alteration of genetic errors at the cellular level. This may further result in thyroid follicular cell proliferation associated with the promotion of TC development.<sup>[20,21]</sup>

A chemically induced rat thyroid tumor model was analyzed by nuclear imaging methods. In our study, PET-CT imaging showed a mean standardized uptake value (SUV) of  $1.58 \pm 0.49$  and  $0.84 \pm 0.14$  [Table 1] in the treated and control groups, respectively [Figure 2a and b], which was statistically significant ( $P = 0.006$ ) suggesting increased thyroid cell metabolism indicating initiation

and propagation of thyroid cells. The F-18 FDG uptake mechanism is based on the cell's basic metabolism and requirement for glucose. Hence, the increased uptake and trapping of deoxyglucose help in demarking the metabolically active area.<sup>[22]</sup> However, variable SUV ( $0.42 \pm 0.17$ ) within the group was observed in the Tc-99 m pertechnetate thyroid scan [Figure 2c and d], with uptake value ranging from 0.2 to 0.6 [Table 1]. Nevertheless, the single animal uptake value in the treatment group was similar to the control ( $0.21 \pm 0.01$ ). This variation may be due to different developmental initiation or propagation of thyroid cells within individual animals. Further, DHPN reacts with targeted tissue and sensitive tissue like the thyroid in initiation and propagation that occurs at the cellular level. All cells show variation in sensitivity and develop preneoplastic tissue alteration at stages such as inflammation, hyperplasia, adenoma, and carcinoma.<sup>[14]</sup> This could be the reason for the variable uptake seen in the different treatment groups of animals.

I-131 uptake by scintigraphy imaging showed thyroid uptake values of  $2.22 \pm 0.34$  and  $2.24 \pm 0.24$  [Table 2] in a few treated and control groups, respectively. Nonetheless, one of the treatment animals showed an uptake of 2.96, due to which a significant difference was not observed between the two groups. However, reduced I-131 SUV ( $2.01 \pm 0.19$ )

was seen in a few DHPN-induced animals ( $n = 4$ ) compared to control animals [Table 3], which may be due to the dedifferentiation of thyroid cells [Figure 2e and f].<sup>[23]</sup> These observations were further confirmed after 20 weeks with HP of the thyroid tissue. Overall, in our preclinical study, the incidence of TC in DHPN-treated animals was around 33%. Up to 50% and 20% incidence of thyroid tumors in the Sprague–Dawley (with short latent intervals of 23 weeks for adenomas and 26 weeks for carcinomas) and medical research council (MRC) rats, respectively, have been reported. In the absence of promoting agent, DHPN has been shown to initiate thyroid tumors with lower frequency. Markedly, there is a difference in the sensitivity of rat strains to this agent.<sup>[24]</sup> On the contrary, the spontaneous incidence of thyroid adenoma in laboratory Wistar rats has been reported as 4.32%.<sup>[25]</sup>

Histopathological examination of the rat thyroid gland showed the development of a thyroid tumor model with adenoma and adenocarcinoma in the animals. Thyroid carcinoma with the characteristic proliferation of follicular to the papillary pattern and an increase in mitotic figures with distant metastasis in the lung and trachea indicate the metastatic adenocarcinoma of the thyroid gland [Figure 3a and b]. A follicular cell pattern was seen suggestive of thyroid adenoma. Imai *et al.*<sup>[17]</sup> have reported tissue HP revealing hyperplastic papillary proliferation of thyroid cells with an increase in numbers and mitotic figures. Further, reduced pendrin expression was seen in DHPN-treated thyrocytes compared to the control [Figure 3c and d]. Reduced pendrin expression was monitored by the gold-standard method IHC, which provides insights into the expression of functional proteins;

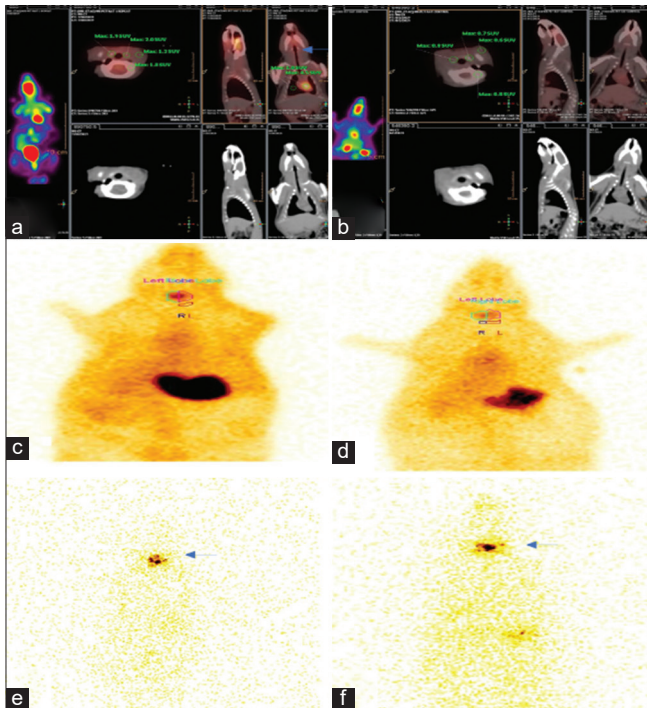


Figure 2: (a) PET-CT scan of the thyroid (arrow) in DHPN-treated animal, (b) PET-CT scan of thyroid in the control animal, (c) Tc-99m scintigraphy scan of the thyroid gland in the treated group with an increased uptake, (d) Tc-99m scintigraphy scan of the thyroid gland in control, (e) I-131 Scintigraphy scan of the thyroid gland in the treated group with reduced uptake, (f) I-131 scintigraphy scan of the normal thyroid gland in control. PET-CT: Positron emission tomography with computed tomography, DHPN: N-bis(2-hydroxypropyl) nitrosamine, Tc-99: technetium-99m, I-131: iodine-131

**Table 1: Positron emission tomography with computed tomography imaging and scintigraphy uptake**

Parameter	PET-CT scan (n=6)		Scintigraphy scan (n=6)	
	Treatment	Control	Treatment	Control
Mean±SD	1.58±0.49	0.84±0.14	0.42±0.17	0.21±0.01

SD: Standard deviation, PET-CT: Positron emission tomography with computed tomography

**Table 2: Iodine-131 uptake**

Parameter	Total animals (n=12)	Control
Mean±SD	2.22±0.34	2.24±0.24

SD: Standard deviation

**Table 3: Animals with reduced iodine-131 uptake**

Animal number	Iodine-131 uptake in individual animal (n=4)
1	2.23
2	1.8
3	1.91
4	2.1
Mean±SD	2.01±0.192006944

SD: Standard deviation

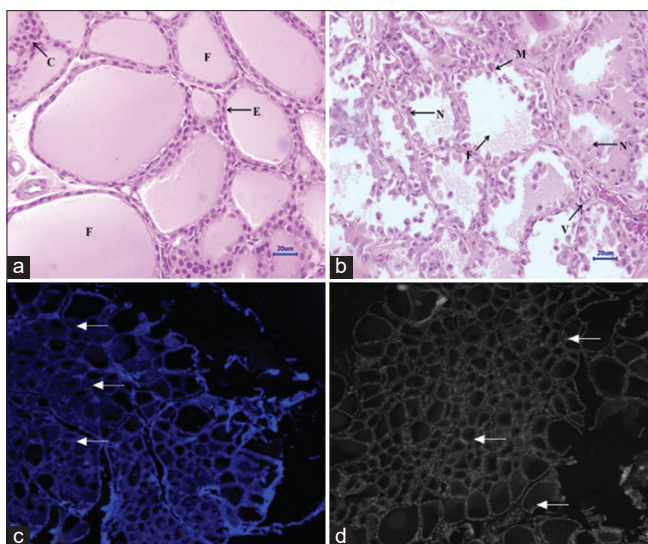


**Figure 3:** (a) Histopathology of the thyrocytes of the control animal with normal follicles (F) with colloidal secretion and lining epithelium (E), few C cells (C) with (H and E,  $\times 40$ ), (b) thyrocytes with follicular to the papillary pattern (N) of the thyroid cell (F), with mitotic figures (M) and new blood vessel formation (V) stained with (H and E,  $\times 400$ ), (c) immunohistochemical expression of thyrocytes with reduced pendrin expression (arrow) at the apical membrane in the DHPN-treated group ( $\times 200$ ), (d) immunohistochemical expression of thyrocytes with normal pendrin expression (arrow) at the apical membrane dark white spot in the control group ( $\times 200$ ). DHPN: N-bis(2-hydroxypropyl) nitrosamine, H and E: Hematoxylin and eosin

and their localization in normal and diseased thyroid tissues which go hand in hand with the reduced I-131 uptake.

In the present IHC study in the animals, polyclonal antiserum against pendrin specifically reacted with the apical membrane of normal follicular cells. Staining for pendrin and apical iodine transporter is limited to the apical membrane.<sup>[26]</sup> This finding supports the hypothesis that pendrin is an apical porter of chloride/iodide. Further, IHC when combined with real-time kinetic quantitative polymerase chain reaction can improve the reliability and accuracy of the results.

A chemically induced TC animal model was successfully developed and confirmed by HP. Nuclear PET-CT and scintigraphy imaging techniques provide additional understanding during the development of the animal model by utilizing a minimum number of laboratory animals, thereby following the principles of the 3Rs.

## Conclusions

Induction of thyroid tumorigenesis was confirmed by traditional HP with advanced nuclear imaging techniques. Further confirmation of neoplastic thyroid tissue alteration was supported by IHC showing reduced pendrin expression in the DHPN-induced TC rat model.

This was further endorsed by I-131 uptake studies, which are well-established methods in human TC diagnosis. In conclusion, nuclear imaging techniques can be used as an additional aid in the development and confirmation

of animal models in laboratory animals. Furthermore, extensive studies need to be carried out on modulating the functional expression of the transport system to induce recovery of I-uptake by TC cells with decreased or absent expression of pendrin. The use of demethylating agents for restoring pendrin expression can be taken as a future perspective. This would help in deciding an effective treatment modality for the patients, which would be contributing significantly to patient life expectancy.

## Acknowledgments

The authors express sincere gratitude to all the staff from the Animal House Facility at the Radiation Medicine Centre, BARC, for their assistance during the experimental work. This study was supported by the Bhabha Atomic Research Centre, Mumbai, India.

## Financial support and sponsorship

Nil.

## Conflicts of interest

There are no conflicts of interest.

## References

- Hu J, Yuan IJ, Mirshahidi S, Simental A, Lee SC, Yuan X. Thyroid carcinoma: Phenotypic features, underlying biology and potential relevance for targeting therapy. *Int J Mol Sci* 2021;22:1950.
- Aashiq M, Silverman DA, Na'ara S, Takahashi H, Amit M. Radioiodine-refractory thyroid cancer: Molecular basis of redifferentiation therapies, management, and novel therapies. *Cancers (Basel)* 2019;11:1382.
- Czarnocka B. Thyroperoxidase, thyroglobulin,  $\text{Na}^+/\text{I}^-$  symporter, pendrin in thyroid autoimmunity. *Front Biosci (Landmark Ed)* 2011;16:783-802.
- Bizhanova A, Kopp P. Minireview: The sodium-iodide symporter NIS and pendrin in iodide homeostasis of the thyroid. *Endocrinology* 2009;150:1084-90.
- Calil-Silveira J, Serrano-Nascimento C, Nunes MT. Iodide treatment acutely increases pendrin (SLC26A4) mRNA expression in the rat thyroid and the PCC13 thyroid cell line by transcriptional mechanisms. *Mol Cell Endocrinol* 2012;350:118-24.
- Kondo T, Nakamura N, Suzuki K, Murata S, Muramatsu A, Kawaoi A, *et al.* Expression of human pendrin in diseased thyroids. *J Histochem Cytochem* 2003;51:167-73.
- Yoshida A, Hisatome I, Taniguchi S, Shirayoshi Y, Yamamoto Y, Miake J, *et al.* Pendrin is a novel autoantigen recognized by patients with autoimmune thyroid diseases. *J Clin Endocrinol Metab* 2009;94:442-8.
- Bidart JM, Mian C, Lazar V, Russo D, Filetti S, Caillou B, *et al.* Expression of pendrin and the Pendred syndrome (PDS) gene in human thyroid tissues. *J Clin Endocrinol Metab* 2000;85:2028-33.
- Arturi F, Russo D, Bidart JM, Scarpelli D, Schlumberger M, Filetti S. Expression pattern of the pendrin and sodium/iodide symporter genes in human thyroid carcinoma cell lines and human thyroid tumors. *Eur J Endocrinol* 2001;145:129-35.
- Xing M, Tokumaru Y, Wu G, Westra WB, Ladenson PW, Sidransky D. Hypermethylation of the Pendred syndrome gene

- SLC26A4 is an early event in thyroid tumorigenesis. *Cancer Res* 2003;63:2312-5.
11. Ormandy EH, Dale J, Griffin G. Genetic engineering of animals: Ethical issues, including welfare concerns. *Can Vet J* 2011;52:544-50.
  12. Hoenerhoff MJ, Hong HH, Ton TV, Lahousse SA, Sills RC. A review of the molecular mechanisms of chemically induced neoplasia in rat and mouse models in national toxicology program bioassays and their relevance to human cancer. *Toxicol Pathol* 2009;37:835-48.
  13. Zhang J, Zhang X, Li Y, Zhou Z, Wu C, Liu Z, *et al.* Low dose of Bisphenol A enhance the susceptibility of thyroid carcinoma stimulated by DHPN and iodine excess in F344 rats. *Oncotarget* 2017;8:69874-87.
  14. Moreira EL, de Camargo JL, Rodrigues MA, Barbisan LF, Salvadori DM. Dose- and sex-related carcinogenesis by N-bis(2-hydroxypropyl) nitrosamine in Wistar rats. *Jpn J Cancer Res* 2000;91:368-74.
  15. Hiasa Y, Kitahori Y, Kitamura M, Nishioka H, Yane K, Fukumoto M, *et al.* Relationships between serum thyroid stimulating hormone levels and development of thyroid tumors in rats treated with N-bis-(2-hydroxypropyl) nitrosamine. *Carcinogenesis* 1991;12:873-7.
  16. Pawar Y, Bhartiya U, Rakshit S, Nandy S, Lakshminarayanan N, Banerjee S. Diagnosis of pathological conditions in laboratory animals by using advance nuclear medicine imaging techniques. *Indian J Vet Pathol* 2019;43:109-14.
  17. Imai T, Onose J, Hasumura M, Ueda M, Takizawa T, Hirose M. Sequential analysis of development of invasive thyroid follicular cell carcinomas in inflamed capsular regions of rats treated with sulfadimethoxine after N-bis(2-hydroxypropyl) nitrosamine-initiation. *Toxicol Pathol* 2004;32:229-36.
  18. Nakano-Narusawa Y, Yokohira M, Yamakawa K, Ye J, Tanimoto M, Wu L, *et al.* Relationship between lung carcinogenesis and chronic inflammation in rodents. *Cancers (Basel)* 2021;13:2910.
  19. Hiasa Y, Kitahori Y, Kato Y, Ohshima M, Konishi N, Shimoyama T, *et al.* Potassium perchlorate, potassium iodide, and propylthiouracil: Promoting effect on the development of thyroid tumors in rats treated with N-bis(2-hydroxypropyl)-nitrosamine. *Jpn J Cancer Res* 1987;78:1335-40.
  20. Mitsumori K, Onodera H, Takahashi M, Shimo T, Yasuhara K, Kitaura K, *et al.* Effect of thyroid stimulating hormone on the development and progression of rat thyroid follicular cell tumors. *Cancer Lett* 1995;92:193-202.
  21. Kim DJ, Han BS, Ahn B, Hasegawa R, Shirai T, Ito N, *et al.* Enhancement by indole-3-carbinol of liver and thyroid gland neoplastic development in a rat medium-term multiorgan carcinogenesis model. *Carcinogenesis* 1997;18:377-81.
  22. Pajak B, Siwiak E, Soltyka M, Priebe A, Zieliński R, Fokt I, *et al.* 2-Deoxy-d-Glucose and its analogs: From diagnostic to therapeutic agents. *Int J Mol Sci* 2019;21:234.
  23. Saha GB. *Fundamentals of Nuclear Pharmacy*. 7<sup>th</sup> 0065d. New York: Springer; 2004.
  24. Boltze C. Animal models of thyroid carcinogenesis. *Cancer Treat Res* 2004;122:273-93.
  25. Isobe K, Mukaratirwa S, Petterino C, Bradley A. Historical control background incidence of spontaneous thyroid and parathyroid glands lesions of rats and CD-1 mice used in 104-week carcinogenicity studies. *J Toxicol Pathol* 2016;29:201-6.
  26. Faggiano A, Caillou B, Lacroix L, Talbot M, Filetti S, Bidart JM, *et al.* Functional characterization of human thyroid tissue with immunohistochemistry. *Thyroid* 2007;17:203-11.